

Lateral spreading in the Canterbury earthquakes - Observations and empirical prediction methods

H.J. Bowen, M.E. Jacka, S. van Ballegooy & T.J.E. Sinclair

Tonkin & Taylor Ltd, New Zealand

H.A. Cowan

New Zealand Earthquake Commission



SUMMARY:

The recent large earthquakes in Canterbury, New Zealand have caused significant damage to tens of thousands of houses across the Canterbury region. The most severe damage to houses was often associated with liquefaction-induced lateral spreading. The occurrence, magnitude and distribution of lateral spreading was different for each major earthquake in the sequence, and was dependent on a number of different factors such as ground shaking intensity, liquefaction susceptibility, topography and geological conditions.

Lateral spreading observations are summarised for two events, the M_w 7.1 earthquake of 4 September 2010 and M_w 6.2 earthquake of 22 February 2011. Data was collected from a variety of sources, including extensive post-earthquake mapping, pre- and post- earthquake LiDAR scanning, and crack width mapping. Information from an extensive geotechnical investigation and strong motion records was used to compare the observed lateral spread to predictions of a widely used empirical method (Youd et al., 2002). Lateral spread displacements were found to be highly dependent on geological and topographical features, and for this case study empirical methods generally over-predicted lateral spread displacement magnitude at large distances from the free face.

Keywords: liquefaction, lateral spreading, Christchurch earthquakes, image coregistration

1. INTRODUCTION

Lateral spreading was a major cause of damage in the recent Canterbury earthquake sequence; the eastern suburbs in particular incurred severe damage to houses, bridges, underground services and roads. Despite the significant economic impact of lateral spreading, the phenomenon is not well understood, and design methods are necessarily approximate in nature due to large aleatoric uncertainties inherent in both the nature of the ground conditions and of earthquake shaking. The objective of this paper is to summarise observations from this earthquake sequence, as part of a longer-term goal of enhancing design methods.

This series of earthquakes has subjected liquefaction-susceptible soils in the region to four strong events, each with different characteristics varying significantly across the city. Combined with detailed mapping of observations, numerous strong motion records and extensive geotechnical investigations, analysis of these earthquakes provides an opportunity to examine key aspects of lateral spreading. Three such aspects are discussed in this paper: the triggering of lateral spreading, the displacement pattern and extent of lateral spreading and the magnitude of lateral spreading displacements.

2. GEOLOGICAL SETTING

Christchurch is located on the east coast of New Zealand's South Island. Figure 1 shows a broad overview of the primary geological units in Christchurch; it can be seen that the city is founded on the boundary of alluvial Springston Formation and the marine Christchurch Formation.

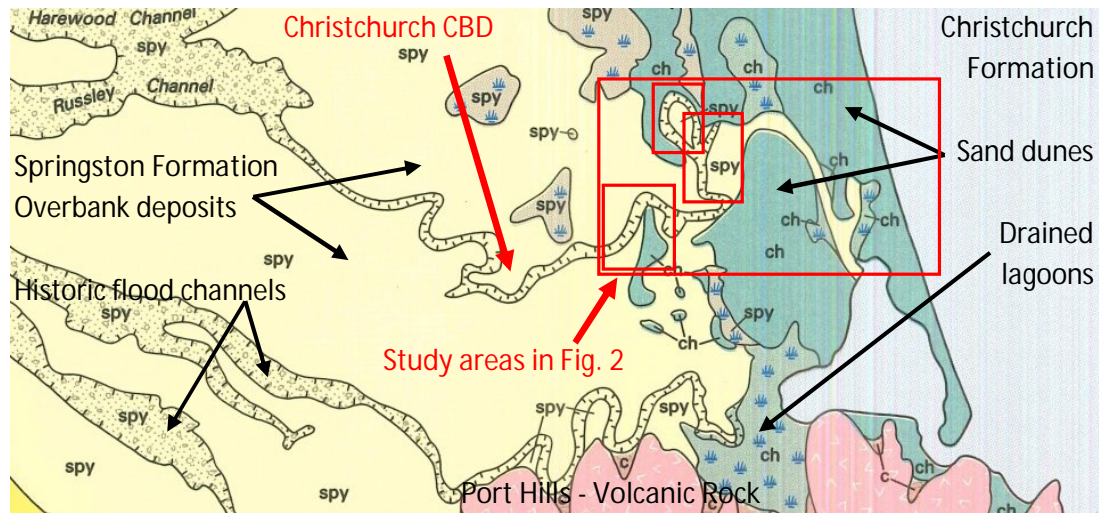


Figure 1 – Map of Christchurch showing primary geological units – Springston Formation (spy) in yellow and the Christchurch Formation (ch) in green (from Brown and Weeber 1992)

The Springston Formation comprises post- glacial fluvial channel and overbank sediments, with three distinct units, (1) alluvial overbank silt which becomes sandy closer to the coast, (2) flood channels infilled with gravel, and (3) peat deposits of former swamps. The Christchurch Formation comprises beach dune sands, and silts and sands from estuarine, lagoonal and coastal swamp deposits. These units are derived from material from the Southern Alps, transported out to sea by the Waimakariri River located to the north of the city.

3. CANTERBURY EARTHQUAKE SEQUENCE

Since the M_w 7.1 earthquake occurred on 4 September 2010, a sequence of significant earthquakes has struck the greater Christchurch region, as summarised in Table 1. All four earthquakes caused lateral spreading to some degree; the most damaging earthquake occurred on 22 February 2011.

Table 1 – Summary of major earthquakes and recorded ground motions in the Canterbury earthquake sequence

Earthquake	Moment magnitude, M_w	Distance from epicentre in eastern suburbs	Typical horizontal PGA in eastern suburbs
4 September 2010	7.1	40 – 42km	0.16 – 0.23g
22 February 2011	6.2	6 – 10km	0.22 – 0.67g
13 June 2011	6.0	7 – 10km	0.22 – 0.46g
23 December 2011	5.9	4 – 6km	0.30 – 0.32g

4. TRIGGERING OF LATERAL SPREADING

Figure 2 compares the extent of lateral spreading that occurred in the 4 September 2010 and 22 February 2011 earthquakes. It can be seen that 22 February earthquake caused lateral spreading to occur in areas that did not suffer spreading in September. Land that underwent lateral spreading in September was the worst affected in February. Of particular interest are sites where liquefaction occurred in both earthquakes, but lateral spreading occurred in February but not September. One such case study is in the suburb of Avondale; two sites labelled A and B in Figure 2.

Site investigations indicate the soil profile is similar across Avondale, with 8-9m of Springston Formation silt and sand overlying denser Christchurch Formation sand. The soil profile at sites A and B comprises low plasticity sandy silt from 0 to 3m below ground level, overlying fine grained loose to medium-dense sand with trace silt from 3 to 9m, overlying dense sands from 9m depth. Both sites are a similar distance from the riverbank, the height of the riverbank and the depth of the river is similar at

both sites. The key difference is the density of the intermediate sand layer – at Site A the sand is loose with CPT tip resistance varying from $q_c = 2\text{-}4\text{MPa}$. At Site B the sand is medium dense, with $q_c = 4\text{-}8\text{MPa}$, as shown in Figure 3.

Analysis indicates that the factor of safety (FOS) against liquefaction, calculated using the method of Idriss and Boulanger (2008), is lower at Site A than Site B. Table 2 summarises the results, which indicate that the observed lateral spread correlates well with the FOS against liquefaction. This suggests that for this case study rapid and complete liquefaction of a soil layer is required for lateral spread to occur. Note that conventional Newmark sliding block analysis with post-liquefaction soil strength would suggest both Sites A and B would undergo lateral spread in the September earthquake.



Figure 2 - Map of eastern Christchurch indicating the extent of liquefaction induced lateral spreading: (a) 4 September 2010 earthquake, with detail locations in Figure 5; (b) 22 February 2011 earthquake

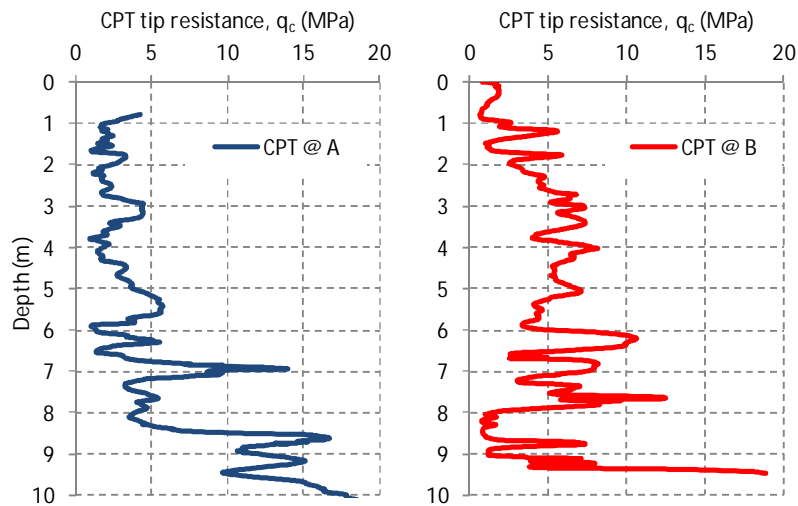


Figure 3 – Cone Penetration Test results at two locations in the suburb of Avondale. At location A lateral spreading occurred in both the 4-Sep-2010 and 22-Feb-2011 earthquakes; at location B lateral spreading occurred in February only, despite liquefaction also occurring in September.

Table 2 – Calculated factor of safety against liquefaction in critical layer at Sites A and B

Site	4 September 2010 Mw=7.1, PGA=0.19g	22 February 2011 Mw=6.2, PGA=0.37g
A	FOS = 0.5 – 0.6	FOS = 0.4 – 0.5
B	FOS = 0.8 – 1.0	FOS = 0.6 – 0.8

5. LATERAL SPREADING DISPLACEMENT PATTERNS & EXTENT

After each of the four main events to date in the Canterbury earthquake sequence, LiDAR survey of ground levels was undertaken to provide information to assist recovery efforts. By comparing the digital elevation models from before and after earthquake events, a pattern-matching image coregistration process was applied to estimate the horizontal ground movements which have occurred. This work was commissioned by EQC and undertaken by Imagin' Labs Corporation and GNS Science, refer to Leprince et al. (2007) for details of this analysis technique. This provides estimated horizontal ground movements from each earthquake, on a 4m grid across much of the Greater Christchurch urban area. By combining the absolute ground movement from the LiDAR analysis with the regional tectonic movements from a fault rupture model, an estimate was made of the local component of ground movement (caused by lateral spreading and other local forms of permanent ground displacement).

As one method for ground-truthing the horizontal displacements from the LiDAR analysis, the displacements were compared to the ground-based mapping of post-earthquake observations on each individual property, as summarised in Figure 4 for the 22-Feb-2011 earthquake. It should be noted that these properties are generally set back from the river's edge – the LiDAR analysis and observation indicates that greater ground displacements occurred in the road and reserve land closer to the free-face. The following observations can be made from Figure 4:

- The LiDAR analysis indicates large local horizontal ground displacements (typically 150 – 700mm) on properties where ground-based mapping identified that severe lateral spreading had occurred. This magnitude of displacement is in general agreement with the ground cracking observed in these areas.

- Moderate local horizontal ground displacements (typically 100 – 500mm) are indicated for properties with severe liquefaction (likely due to ground-oscillation or sloping-ground effects) and moderate lateral spreading (likely due to free-face effects). This magnitude of displacement is in general agreement with the ground cracking observed in these areas.
- The analysis indicates minor local horizontal displacements (typically 100 – 300mm) for properties with moderate, minor and no liquefaction observed. This magnitude of displacement is greater than implied by the limited ground cracking observed in these areas. Much of the displacement indicated by the analysis is likely to be noise, due to the limited accuracy of the LiDAR data and tectonic model. However some of this displacement may be real, associated with minor cyclic seismic displacements within the deep soil profile, slope movement, or similar effects not associated with lateral spreading.

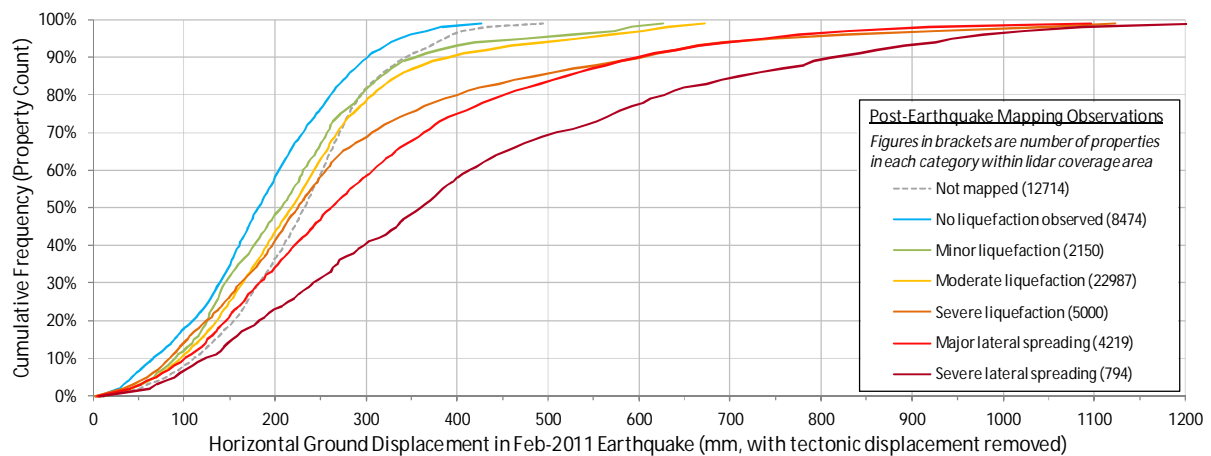


Figure 4 – Correlation between ground-based post-earthquake mapping and displacement from LiDAR analysis, for 22 February 2011 earthquake.

Figure 5 presents results from the analysis of LiDAR data for three areas within the eastern suburbs of Christchurch. Figure 6 summarises the observed trends of reducing ground displacement with distance away from the free edge. The ground displacement patterns in each of these areas show a number of different effects as discussed below.

Figure 5(a) shows the suburbs of Richmond, Avonside and Dallington, with the Avon River meandering through the centre. The ground elevation map on the left clearly shows the position of river terraces and lower-lying point bar deposits. The map on the right shows the magnitude of local horizontal displacement that occurred due to the 22 February 2011 earthquake (after correction to remove the tectonic component of ground movement). Ground movement is predominantly directly towards the nearest riverbank, driven by both free-edge effects and the moderately-sloping topography. It can be seen that in this area, the most significant lateral spreading ground displacements are generally constrained within the boundaries of the lower river terraces. It is inferred that on the upper terraces, where significant lateral spreading was not observed despite widespread liquefaction occurring, the denser soils suffered less-severe strength loss following liquefaction triggering.

Figure 5(b) shows that the suburb of Avondale (to the east of the river) is predominantly near-flat low-lying land, with some higher ground to the south and north. In the near-flat region (0.1 – 0.2% slope) there appear to be no distinct topographical or geological constraints to the lateral spreading ground movements (the nearest significant change is the higher and denser dune deposits about 700m to the east, just off the edge of the map). Lateral ground movements appear to be driven predominantly by

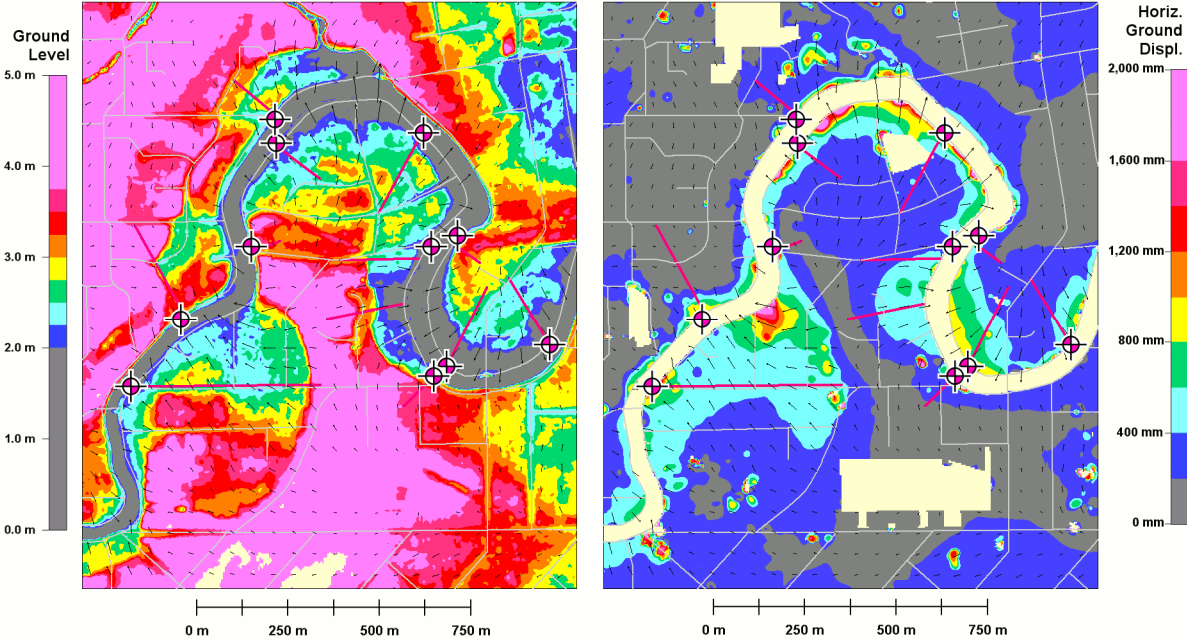
free-face effects, with little effect from inland topography. Without constraints, the magnitude of ground displacement reduces gradually with distance back from the free-face over a width of about 150 – 200m (beyond this distance any lateral spreading toward the free-face is lost in the background noise and other forms of ground movement). In the northern and southern areas, minor lateral ground movements extend further inland, driven by the more steeply-sloping higher ground.

Figure 5(c) shows the suburb of Horseshoe Lake, which is surrounded by an oxbow lake from the historic meandering river channel. The lowest-lying land in the southeast is approximately 1.2m below the higher ground in the northwest and southwest, and 0.6m below the ground in the west (ground slope of 0.1 – 0.2%). Along the western and northern reaches of the lake, lateral spreading has occurred towards the nearby free-face only in areas which are very close to the edge. The predominant driver of lateral ground movement across the majority of the Horseshoe Lake suburb appears to be the overall ground topography sloping towards the low-lying south eastern area.

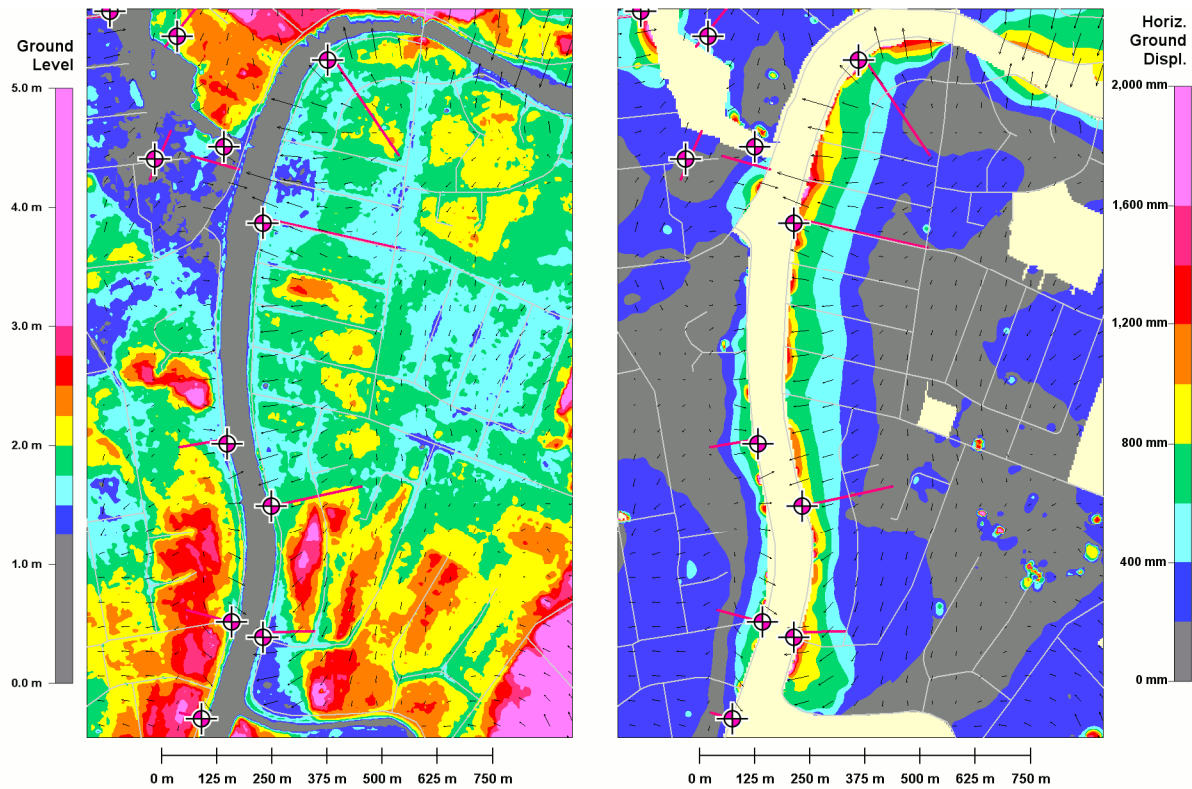
6. MAGNITUDE OF LATERAL SPREADING DISPLACEMENTS

The magnitude of the lateral spreading displacements obtained from the LiDAR survey as described in Section 5 was compared with a widely used empirical method for predicting lateral spreading displacements (Youd et al. 2002). The measured displacements have been baseline-corrected to zero once the displacement profile reaches a near-constant value – this is intended to isolate the component of ground movement associated with lateral spreading towards the free edge, filtering out the noise and other types of ground movement present in the data.

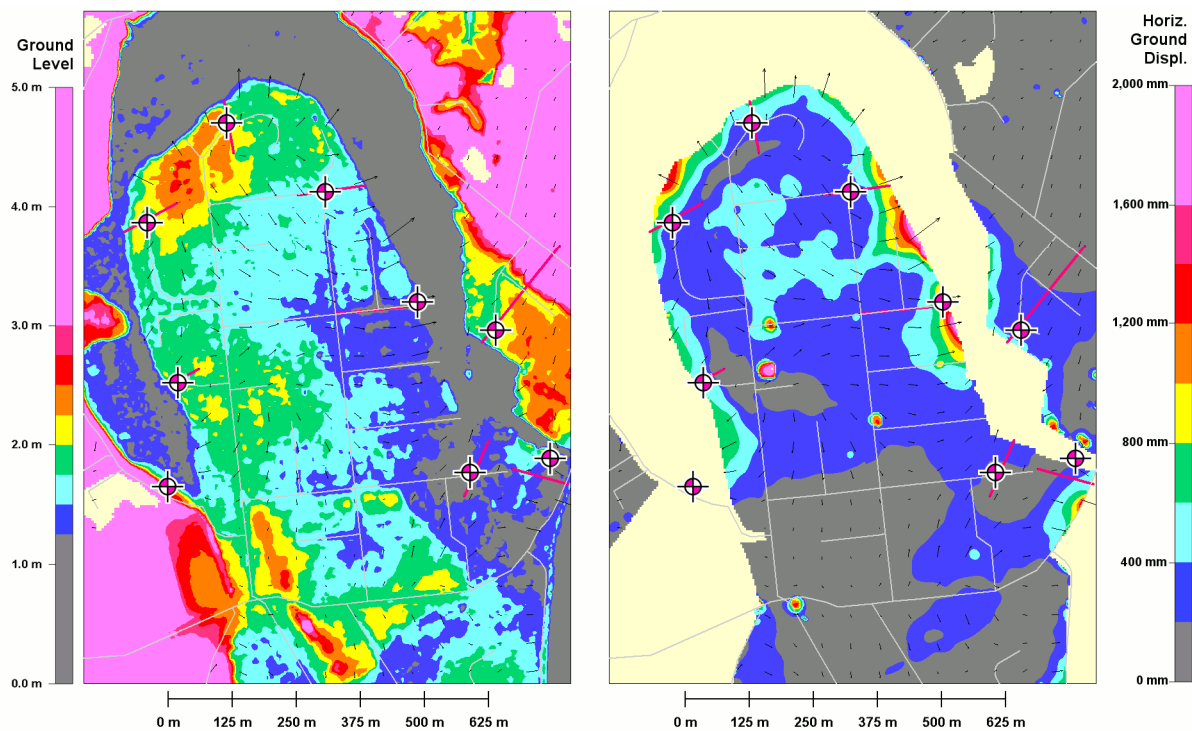
The predicted displacement was determined for the 22 February 2011 earthquake using information from a comprehensive post- earthquake geotechnical investigation. 28 boreholes were drilled alongside the Avon River in areas affected by lateral spreading, the location of these boreholes are shown in Figure 2 and Figure 5. In addition, hundreds of CPTs and kilometres of MASW geophysical survey lines were also undertaken in these areas. Table 3 summarises the sources of key information used in this assessment.



(5a) Avonside



(5b) Avondale



(5c) Horseshoe Lake

Figure 5 – LiDAR analysis for selected suburbs of eastern Christchurch. Left image is LiDAR elevation survey; changes in elevation correspond to the presence of different geological units such as river terraces or sand dunes. Right image shows the magnitude (colours) and direction (vectors) of lateral spreading displacements, calculated from the difference between pre- and post- earthquake LiDAR surveys for the 22 February 2011 earthquake.

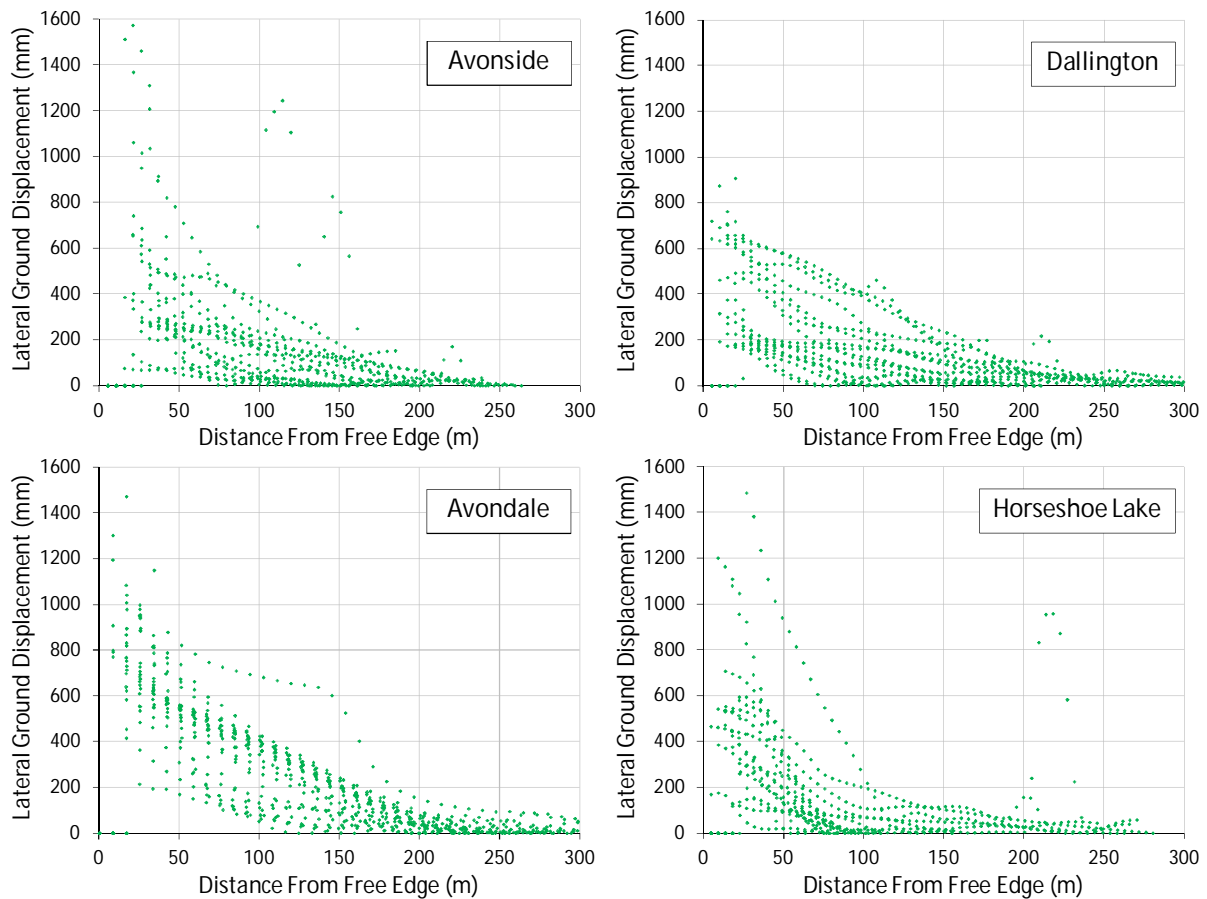


Figure 6 – Observed displacement vs. distance profiles for selected suburbs, derived from LiDAR analysis. Displacement profiles have been baseline-corrected to zero displacement at the minimum point – to isolate the component of ground movement associated with lateral spreading towards the free edge (filtering out the noise and other types of ground movement present in the data).

Table 3 – Parameters used in Youd et al. (2002) method

Parameter	Information source
Magnitude, M	$M = 6.2$
Source distance, R	Determined two ways: (a) R = actual distance from earthquake epicentre (b) $R = R_{eq}$, equivalent source distance calculated using peak ground accelerations recorded nearby
Height of free face, H	LiDAR survey and pre- earthquake riverbed survey
Thickness of liquefiable deposit, T_{15}	SPT testing in boreholes adjacent to the Avon River
Average fines content, F_{15}	Laboratory tests
Average mean grain size, $D_{50_{15}}$	Laboratory tests & interpretation from logged soil description

The Youd et al. Method was developed for western U.S. and Japan where attenuation of seismic waves is relatively high. For other seismic regions, Youd et al. recommend the use of an equivalent source distance, which is determined using attenuation models that incorporate the earthquake magnitude and the peak ground acceleration. In general, the peak ground accelerations experienced in eastern Christchurch were much higher than conventional attenuation models suggest. Therefore, for the purposes of this paper, both the equivalent source distance (calculated using the observed peak ground accelerations recorded nearby) and the actual source distance were used to prepare predictions. Figure 7 compares the predicted and observed displacements. In general, displacements immediately next to the free edge are affected by instability and are difficult to predict. Distances further back are

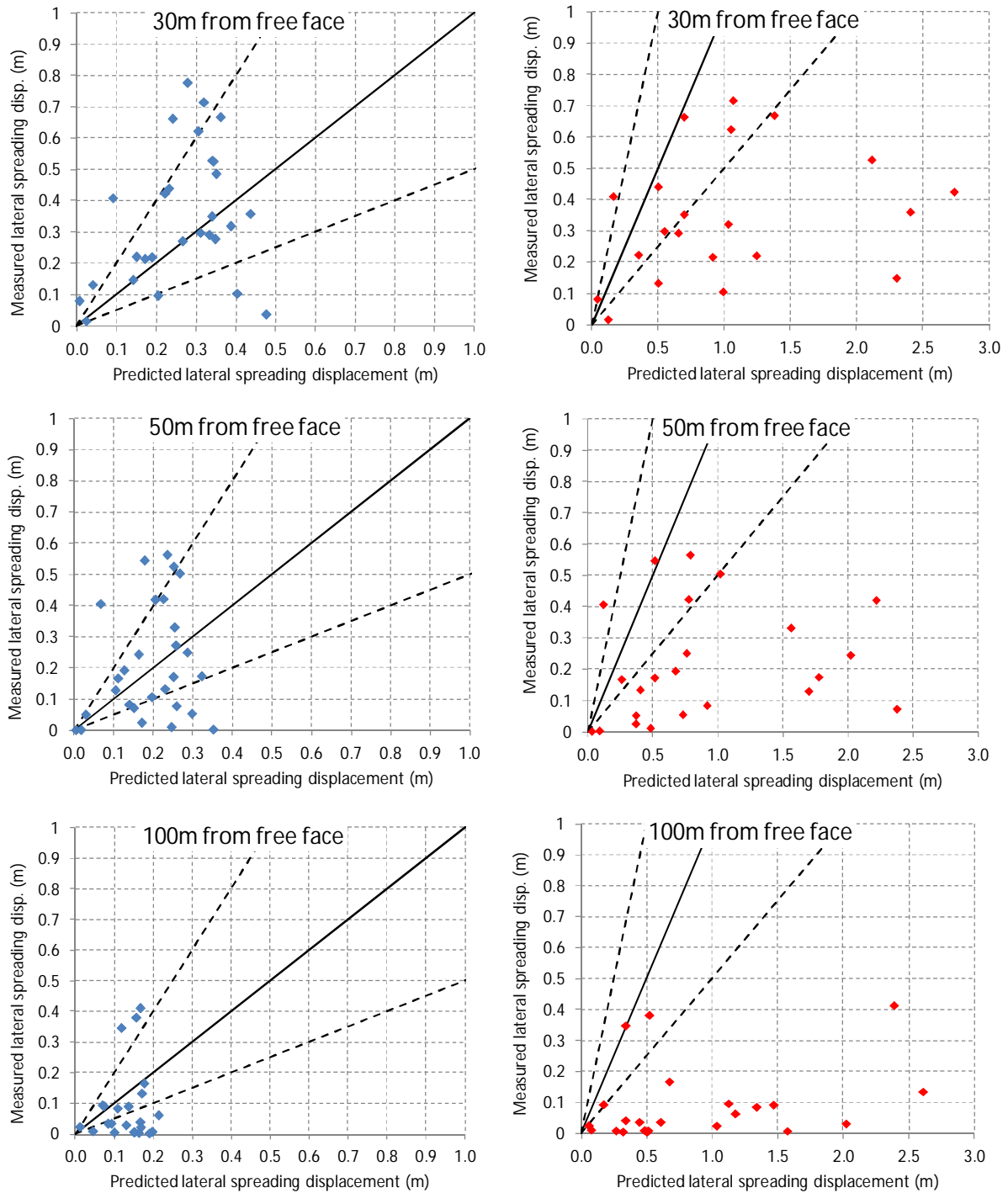


Figure 7 – Comparison of predicted lateral spreading displacement using Youd et al. (2002) versus lateral spreading displacement measured using LIDAR survey. For the plots on the left hand side (blue symbols) the predicted displacements were calculated using the actual distance to the source. On the right hand side (red symbols) the predicted displacements were calculated using the equivalent source distance. The solid line represents predicted displacement = measured displacement, and the top and bottom dashed lines represent predicted displacement = 0.5 times and 2 times the measured displacement respectively. As shown in Figure 6, measured displacement profiles have been baseline-corrected to zero displacement at the minimum point.

typically of more relevance to engineers, so comparisons at 30m, 50m and 100m distance from the free edge are presented. For the plots on the left hand side (blue symbols) the predicted displacements were calculated using the actual distance to the source. On the right hand side (red symbols) the predicted displacements were calculated using the equivalent source distance.

From inspection of the data it can be seen that:

- There is a large amount of scatter in the data, however at 30m and 50m from the riverbank the measured displacements were broadly accurate within a factor of 2 when using the actual source distance.
- Use of the equivalent source distance results in an over-prediction of displacement for these case studies. This may be due to the strong ground motions experienced in this particular earthquake, rather than the prediction model itself. It does demonstrate however that the prediction method is very sensitive to small magnitude earthquakes close to the source.
- For these case studies, the method over-predicts lateral-spreading displacements at larger distances (greater than 100m) back from the riverbank.

7. CONCLUSIONS

This paper provides a summary of observations and preliminary analysis on lateral spreading during the Christchurch earthquakes. Key outcomes from this work include:

- Rapid and complete liquefaction of susceptible layers is required to trigger lateral spreading for this case study of moderate-magnitude earthquakes.
- Geological and topographical features have a great influence on the displacement pattern and extent of lateral spreading.
- Application of various analysis techniques to the LiDAR data provides valuable case-study information that can be used to further develop empirical lateral spreading analysis methods.
- Displacements predicted by the Youd et al. method were greater than measured displacements at large distances from the free edge for this case study, possibly related to the high PGA experienced close to the fault in this moderate-magnitude earthquake.

ACKNOWLEDGEMENT

This work would not have been possible without the data obtained by the New Zealand hazard monitoring system (GeoNet) and the extensive remote sensing and ground investigations of land damage, sponsored by the New Zealand Government through its agencies the Earthquake Commission of New Zealand, the Ministry of Civil Defence and Emergency Management and Land Information New Zealand.

REFERENCES

- Brown, L.J. and Weeber, J.H. (1992). Geology of the Christchurch Urban Area. Scale 1:25,000. Institute of Geological & Nuclear Sciences Geological Map 1.
- Idriss, I.M. and Boulanger, R.W. (2008). Soil liquefaction during earthquakes. EERI MNO-12.
- Leprince, S., Barbot, S., Ayoub, F. and Avouac, J. P. (2007). Automatic and Precise Ortho-rectification, Coregistration, and Subpixel Correlation of Satellite Images, Application to Ground Deformation Measurements", IEEE Transactions on Geoscience and Remote Sensing, Vol.45, No.6, June 2007.
- Youd, T.L., Hansen, C.M., and Bartlett, S.F., (2002). Revised multi-linear regression equations for prediction of lateral spread displacement, J. Geotechnical and Geoenvironmental Eng. 128(12), 1007-017.